Fabrication of the Shell-type Nb_3Sn Dipole Magnet at Fermilab

Deepak R. Chichili, Giorgio Ambrosio, Nicolai Andreev, Emanuela Barzi, Shlomo Caspi, Vadim V. Kashikhin, Peter J. Limon, Ronald Scanlan, Iouri Terechkine, John Tompkins, Masayoshi Wake, Sunil Yadav, Ryuji Yamada, Victor Yarba, and Alexander V. Zlobin

***Abstract*— A 43.5 mm aperture dipole magnet with a nominal field of 11 T is being fabricated at Fermilab. The design is based on a two-layer shell-type coil structure made of Rutherford-type Nb_3Sn cable with wind and react technology. The mechanical support structure consists of vertically split iron yoke locked by two aluminum clamps and a 8 mm thick stainless steel skin. This paper summarizes the fabrication details of the first dipole model and test results from a 200 mm long mechanical model.**

***Index Terms*—Nb_3Sn, dipole magnet, fabrication**

I. Introduction

TWO years ago Fermilab initiated a High Field Magnet Program to develop a cost effective and reliable Nb_3Sn magnet suitable for a future Very Large Hadron Collider (VLHC). Extensive studies on shell-type designs with various bore diameters, current block arrangements, cable parameters, etc. have been conducted [1]. The results of these studies have culminated into fabrication of the first 1 meter long dipole model. The magnet design is based on the two layer shell-type coil with a 43.5 mm bore and a cold iron yoke (Fig. 1). The details of the design have already been reported [2],[3]. The reacted and impregnated coils are mechanically supported by a vertically split iron yoke locked by two aluminum clamps and surrounded by a 8 mm thick stainless steel skin. The clamps provide the initial preload to the coils as well as aiding in yoke assembly. The final coil prestress at room temperature is provided by both the clamps and the skin. The space between the coils and the yoke is filled with 8 mm thick aluminum spacers. Finally, 50 mm thick end-plates are used to restrict the longitudinal coil motion under the Lorentz forces.

II. Magnet Fabrication

A. Superconducting Strand and Cable

Nb_3Sn strand and cable parameters are listed in Table I. The conductor was manufactured by OST using the Modified Jelly Roll (MJR) process. Keystoned Rutherford type cable with a 25 μm thick stainless steel core was manufactured at LBNL. Both virgin and extracted strand critical parameters have been measured [4]. The critical current density for the virgin strand at 12 T, 4.2 K was measured to be about 2000 KA/mm^2 with a RRR of 30. The degradation due to cabling was measured to be less than 10% for a packing factor of 88.8% [5].

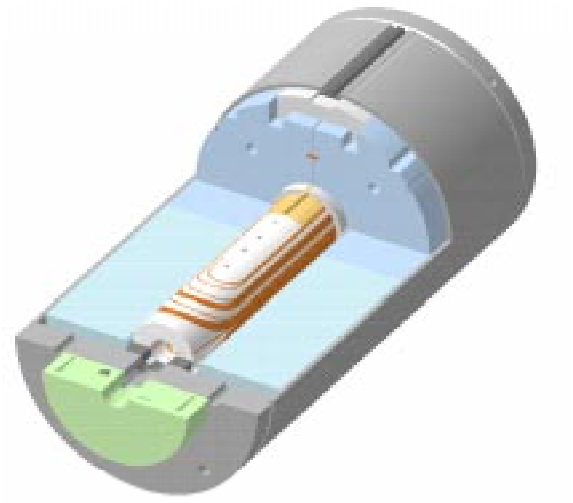

Fig. 1. Two-layer shell-type Nb_3Sn dipole magnet.

TABLE I
Strand and Cable Parameters

Parameter	Unit	Value
Strand Diameter	mm	1.00
Effective Filament Diameter	μm	115
Cu : non Cu ratio		0.92
Cable Width	mm	14.23
Cable Mid-Thickness	mm	1.82
Keystone angle	deg	0.927
Cable Pitch Length	mm	109.8
Number of Strands		28
Cable Lay Direction		Left

B. Coil Fabrication

The cable was first cleaned with a solvent (ABZOL VG) and wrapped with a 50% overlap ceramic tape, CTD CF100. The nominal thickness of the cable insulation is 250 μm. A thin layer of inorganic ceramic matrix, CTD 1002x was applied to the insulated cable using rollers. The entire spool of wet insulated cable was cured at 80 ^{o}C for 20 min. This resulted in cable with a strong insulation system [6].

Manuscript received September 17, 2000. This work was supported by the U.S. Department of Energy.

D. Chichili, G. Ambrosio, N. Andreev, E. Barzi, V. Kashikhin, P. Limon, I. Terechkine, J. Tompkins, S. Yadav, R. Yamada, V. Yarba, and A. Zlobin are with Technical Division, Fermilab, Batavia, IL 60510 USA (telephone: 630-840-4710, e-mail: chichili@fnal.gov).

S. Caspi and R. Scanlan are with LBNL, Berkeley, CA 94720 USA (telephone: 510-486-7244, e-mail: s_caspi@lbl.gov).

M. Wake is with KEK, Tsukuba, Japan (e-mail: wake@post.kek.jp).

Each half coil consisted of 24 turns, 11 turns in the inner layer and 13 turns in the outer layer. Both inner and outer layers were wound with a single length cable thus requiring no interlayer splice. Four wedges per quadrant, two on each layer and floating pole pieces, one on each layer were used to minimize the lower order geometrical harmonics and to ensure radial turn position in the coil. The coil end-parts, wedges and pole pieces were made out of aluminum-silicon bronze, C642. This material was chosen because its melting temperature is high enough to withstand the reaction temperature and its thermal contraction coefficient is similar to that of the coil in the azimuthal direction. The end parts were designed using optimization program BEND [7] and were fabricated at LBNL [8]. After fabrication, end parts were coated with 125 μm thick ceramic coating.

Fig. 2 shows a wound inner coil. Gaps were introduced in the pole pieces and the wedges to account for differential thermal expansion during reaction in the longitudinal direction. Thin strips of stainless steel which act as voltage taps were inserted between the cable and the insulation during winding around the end-parts. After the inner coil was wound, the ceramic matrix was applied along the length of the coil using a brush. The wet coil was then packaged for curing. After initial cycling at low pressures, a final azimuthal pressure of 45 MPa and a radial pressure of 10 MPa was applied to obtain the required coil geometry. The curing temperature of 150 ^{o}C was held for 30 min. The cured coil had good turn-to-turn bonding.

Fig. 2. Inner coil after winding.

Fig. 3. Cured half-coils used in the first dipole model.

The next step in the production of the half-coil was to fabricate and install an interlayer insulation consisting of three layers of ceramic cloth each 125 μm thick. The three layers were preformed into shape using a ceramic matrix and a forming fixture. The middle layer contained two bands of 25 μm thick stainless steel strip heaters for quench protection. The outer layer was wound on top of the cured inner layer and interlayer insulation. The curing of the outer layer was performed along with the previously cured inner layer. This completes the production of a half-coil. Two such half coils as shown in Fig. 3 were fabricated for the first dipole model.

The azimuthal size of the cured half coils were measured at four positions along the length of the straight section at varying pressures. Fig. 4 shows the data with respect to the nominal size. The mean azimuthal size at a pressure of 3 MPa for the first half coil is 0.2 mm and that of second half coil is 0.01 mm over the nominal size. The standard deviation is about 0.07 mm. The insulation overlap of the wedges for the second half coil was reduced from 50% overlap to butt lap to reduce the overall coil size, since we anticipated further increase in size after reaction. The average modulus of elasticity in the azimuthal direction for the cured half coil is about 20 GPa. Electrical measurements were also taken on both the half-coils to check for possible turn-to-turn shorts (inductance, impedance and resistance). The data is given in Table II. Both the coils have similar values and match the theoretical estimates, which indicate that they are free from turn-to-turn shorts.

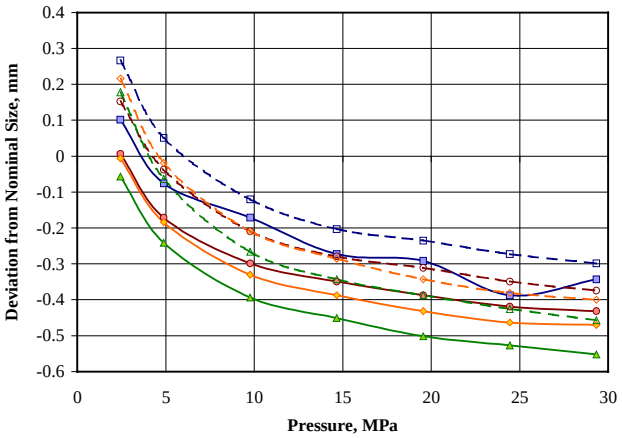

Fig. 4. Azimuthal coil size variation with pressure at four positions. Dashed lines represent the first half coil and solid lines represent the second coil.

C. Coil Reaction

The two half-coils along with the ground insulation were assembled around a stainless steel mandrel and then placed in the reaction fixture. Ground insulation consisted of three layers of 0.125 mm thick ceramic cloth preformed into shape using the ceramic matrix. The ends of the lead cables from the two half coils were welded to prevent tin from leaking during the reaction. The leads were also supported during reaction to prevent any damage. The reaction fixture goes into a retort and the whole assembly is then placed in the furnace. The retort was pumped for several hours and later purged with Argon. The flow rate of Argon was adjusted to be at least 1 cm^3/sec. The reaction process was a two step cycle: 575 ^{o}C for 200 hr. followed by 700 ^{o}C for 40 hr. with a ramp rate of 25 ^{o}C/hr. This thermal cycle was chosen as it gave the best critical current and magnetization properties based on short sample studies [4]. Temperature distribution of the coils was measured throughout the reaction cycle. The deviation between the coil and the furnace temperature decreases with the increase in temperature and is within 1-2 ^{o}C above 500 ^{o}C.

Both mechanical and electrical measurements were taken on the half-coils after reaction. Coil length measurements showed that the coil grew by about 9 mm due to reaction. Since the coil azimuthal size was more than the nominal, additional pressure was applied while tightening the bolts on

the reaction fixture. This might have caused the coils to expand longitudinally during reaction. Azimuthal coil size measurements were not performed on the half coils. Instead, they were done on a practice coil, HFM-PC-02 (Fig. 5). Azimuthal size of a half-coil increases by about 500 μm for pressures less than 15 MPa. For future magnets, the size of the coils before reaction should be 0.5 mm less than the nominal size. Firstly, this will reduce the pressure required to close the reaction fixture and secondly, after reaction the coils will grow to the nominal size.

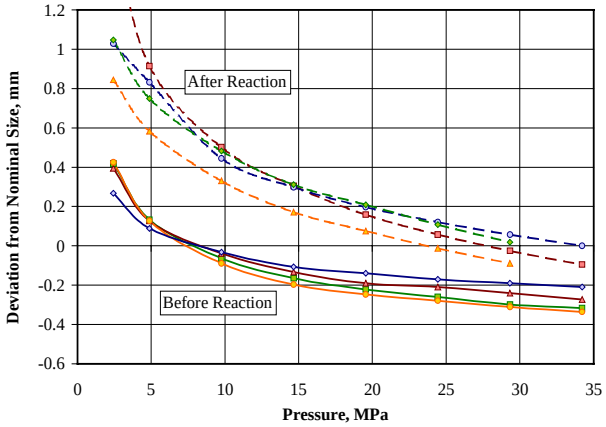

Fig. 5. Azimuthal coil size variation with pressure before and after reaction.

Table II summarizes the electrical data. The resistance of the coil increases with reaction. Furthermore the first half coil has low inductance compared to second half-coil indicating that it has developed shorts during reaction. Tin leakage was found in both the coils after reaction. Turn-to-turn resistance measurements indicated that the shorts in the first half coil were developed near the spots with tin leakage. This observed tin leakage was attributed to the removal of low temperature, 200 ^{o}C step from the reaction cycle where tin diffuses in solid phase, as well as high compaction of coils before reaction. A plan is being developed to investigate this behavior.

TABLE II
ELECTRICAL MEASUREMENTS ON HALF-COILS

Parameter	Before Reaction		After Reaction	
	First Coil	Second Coil	First Coil	Second Coil
Inductance, μH	232.4	236.4	94.3	200.8
Impedance	6.01	6.36	0.93	2.68
Resistance, mΩ	56.5	62.8	78.6	81.9

D. Splice Joints

The Nb_3Sn to NbTi splicing was performed while the coil assembly is still inside the reaction fixture. The Nb_3Sn leads and the splice cables were always supported to prevent any possible damage to the reacted Nb_3Sn strands. The splice assembly consisted of a 0.55 mm thick 125 mm long copper cage, two NbTi cables, one Nb_3Sn lead cable and a 0.55 mm thick 125 mm long copper top plate. The NbTi splice cable was designed to ensure that two NbTi cables along with a Nb_3Sn cable in the middle results in a rectangular cross-section. A brass ring was installed after making the splice joints to support them (Fig. 6).

Fig. 6. Splice Joints with brass ring. See also the supports for splice cables.

E. Epoxy Impregnation

After the splice joints were made, the coil assembly was transferred from the reaction fixture to the impregnation fixture. A roll-over fixture was designed to facilitate this process. This made it possible to remove each half of the reaction fixture and install the corresponding half of the impregnation fixture. A 125 μm thick mold released Kapton layer was inserted between the two half-coils and around them during this transfer. The stainless steel mandrel used during reaction was removed and a Teflon mandrel was installed in its place. Note that the Teflon mandrel has a clearance of 0.5 mm with the inner diameter of the coil. Since the thermal expansion coefficient of Teflon is more than that of the coil, the mandrel diameter was chosen such that during curing, it expands to fill the whole aperture. After cool down it was possible to remove the mandrel. The mold released Kapton layer inserted between the two half-coils also gave the option of splitting the coils after impregnation. CTD-101K epoxy was used to impregnate the coil. Impregnation was carried out at 60 ^{o}C to decrease the viscosity of the epoxy. The process took about 5 hr. The curing cycle involved increasing the temperature to 125 ^{o}C and keeping it there for 20 hr. Fig. 7 shows the impregnated coil structure.

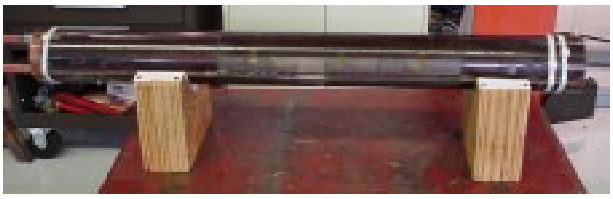

Fig. 7. Epoxy impregnated coil assembly.

F. Instrumentation

The impregnated coil assembly and various components of the magnet were instrumented with gauges to measure the stress during magnet assembly and operation. Four capacitance gauges were installed in the dipole model between the outer pole pieces and the coil to measure the azimuthal stress. Capacitance gauges were fabricated in house and calibrated at room temperature and at 4.2 K. Resistive gauges were installed on structural components like spacers, clamps and skin to measure the stress. The low temperature zero readings for these gauges were obtained by putting the instrumented components in a liquid He bath.

III. Mechanical Model

An eight inch long mechanical model was fabricated to test the magnet assembly procedure and to verify the mechanical analysis. A half-coil was wound, cured, reacted and epoxy impregnated for this purpose. Nb_3Sn cable made out of ITER strand was used with S-2 fiberglass as insulation material. The straight section of the half-coil was cut into two halves and assembled as a mechanical model. Two capacitance gauges were installed between the outer pole piece and the coil to measure azimuthal stress. Two resistive gauges were installed on the aluminum spacer, one near the pole region and one near the mid-plane to measure its azimuthal stress.

The coils and yoke were assembled in the contact tooling (Fig. 8). The yoke halves were then compressed vertically in a press. The aluminum clamps were inserted from the sides with a separate set of pusher blocks. After the clamps were inserted the pump pressure was released and the assembly springs back to an equilibrium position.

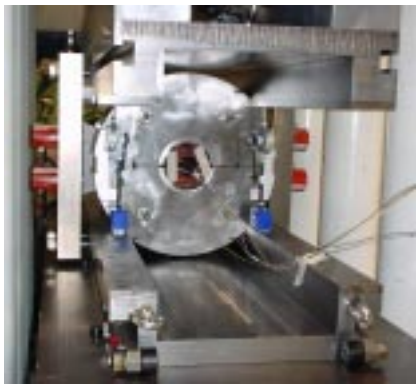

Fig. 8. Magnet yoking/clamping process.

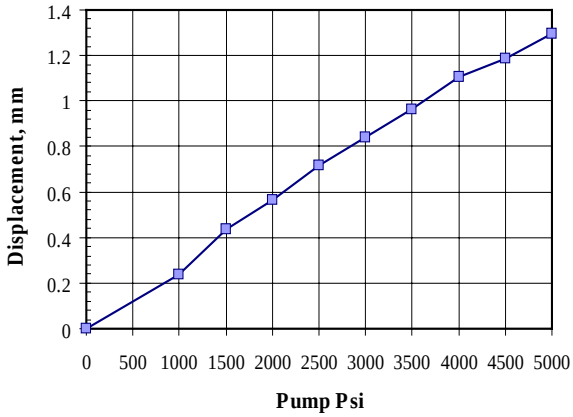

Fig. 9. Displacement of the yoke halves with pressure.

Dial indicators were placed between the two platens that push the yoke halves (see Fig. 8). The pump pressure was increased incrementally (500 Psi steps) and the displacements were noted (Fig. 9). Note that the response was quite linear and the data was very repeatable. This indicates that we are working in a elastic regime of the coil structure. Table III summarizes the gauge data at various stages of the assembly process. The high stresses in the coil during magnet assembly is due to large size of the coil structure. The outer diameter of the epoxy impregnated coil "pipe" is 0.25 mm more than the nominal size. The support structure is designed so that an azimuthal interference exists between the aluminum spacer and the outer pole extension, which prevents the coils from over compressing during assembly. However, the oversize coil structure reduces the interference, thus increasing the transfer of stresses from the spacer to the coil. After spring back, the stress in the coil decreases to about 32 MPa. The is about a third of the required coil pre-stress at room temperature. The rest of it is provided by the skin through weld shrinkage. The estimated values using ANSYS were also included in the table. The model predicts the experimental data reasonably well except for the spacer stress at the mid-plane. This is due to uncertainty in the spacer and outer pole extension interference. The next step is to weld the skin around the yoked assembly. We expect to complete the fabrication of the short model by the middle of October.

TABLE III
Data From the Mechanical Model (MPa)

		Coil Pole	Spacer Mid-Plane	Spacer Pole
Model				
	Under Press	154	88	152
	Under Press + Clamp	156	91	161
	After Spring back	32	40	51
Analysis				
	Under Press	145	122	156
	After Spring back	40	43	50

IV. Conclusions

The fabrication of 1 meter long Nb_3Sn dipole model is underway. The proposed coil fabrication technique resulted in the production of coils with good mechanical properties. Some optimization of coil size and reaction cycle to eliminate tin leakage is being developed. The magnet assembly process has been verified on a short mechanical model. The data from the mechanical model agrees reasonably well with that of the analysis. The fabrication of new coils is in progress and the magnet production is expected to be completed by December.

References

[1] G. Ambrosio et al., "Conceptual design study of high field magnets for very large hadron collider," *IEEE Trans of Applied Superconductivity*, vol. 10, pp. 310-313, March 2000.

[2] G. Ambrosio et al., "Magnetic design of the Fermilab 11 T Nb_3Sn short dipole model," *IEEE Trans of Applied Superconductivity*, vol. 10, pp. 322-325, March 2000.

[3] G. Ambrosio, N. Andreev, D. Chichili et al., "Mechanical design and analysis of the Fermilab 11 T Nb_3Sn dipole model," *IEEE Trans of Applied Superconductivity*, vol. 10, pp. 306-309, March 2000.

[4] E. Barzi et al., "Study of Nb_3Sn strands for Fermilab high field dipole models," *this Conference*.

[5] E. Barzi et al., "Strand critical current degradation in Nb_3Sn Rutherford-type cables," *this Conference*.

[6] D. Chichili et al, "Investigation of cable insulation and thermo-mechanical properties of Nb_3Sn composite," *IEEE Trans of Applied Superconductivity*, vol. 10, pp. 1317-1320, March 2000.

[7] J. M. Cook, "Strain energy minimization in SSC magnet winding," *IEEE Trans. on Magnetics*, vol. 27, pp. 1976-1980, March 1991.

[8] S. Yadav, D. Chichili and I. Terechkine, "Coil design issues for high field dipole model," *this Conference*.